



Published in final edited form as:

Free Radic Biol Med. 2018 October ; 126: 187–201. doi:10.1016/j.freeradbiomed.2018.08.001.

Mechanical stretch induces antioxidant responses and osteogenic differentiation in human mesenchymal stem cells through activation of the AMPK-SIRT1 signaling pathway

Xi Chen^{a,b,c}, Jinku Yan^{a,b}, Fan He^{a,b,*}, Dongyan Zhong^{a,b}, Huilin Yang^{a,b}, Ming Pei^d, and Zong-Ping Luo^{a,b,**}

^aOrthopaedic Institute, Medical College, Soochow University, Suzhou 215007, China

^bDepartment of Orthopaedics, The First Affiliated Hospital of Soochow University, Suzhou 215006, China

^cSchool of Biology and Basic Medical Sciences, Medical College, Soochow University, Suzhou 215123, China

^dStem Cell and Tissue Engineering Laboratory, Department of Orthopaedics, West Virginia University, Morgantown, WV 26506, USA

Abstract

Mesenchymal stem cells (MSCs) are promising cell sources for regenerative medicine. Growing evidence has indicated that mechanical stimuli are crucial for their lineage-specific differentiation. However, the effect of mechanical loading on redox balance and the intracellular antioxidant system in MSCs was unknown. In this study, human bone marrow-derived MSCs (BM-MSCs) were subjected to cyclic stretch at the magnitude of 2.5%, 5%, and 10%. Cell proliferation, intracellular reactive oxygen species (ROS), expression of antioxidant enzymes, and osteogenic differentiation were evaluated. RNA was extracted and subjected to DNA microarray analysis. Sirtinol and compound C were used to investigate the underlying mechanisms involved silent information regulator type 1 (SIRT1) and AMP-activated protein kinase (AMPK). Our results showed that mechanical stretch at appropriate magnitudes increased cell proliferation, up-regulated extracellular matrix organization, and down-regulated matrix disassembly. After 3 days of stretch, intracellular ROS in BM-MSCs were decreased but the levels of antioxidant enzymes,

* **Corresponding Author:** Fan He, Ph.D., Orthopaedic Institute, Medical College, Soochow University, No.708 Renmin Road, Suzhou 215007, Jiangsu, China. Telephone: +86-512-67781420; Fax: +86-512-67781165, fanhe@suda.edu.cn. ** **Corresponding Author:** Zong-Ping Luo, Ph.D., Orthopaedic Institute, Medical College, Soochow University, No.708 Renmin Road, Suzhou 215007, Jiangsu, China. Telephone: +86-512-67781351; Fax: +86-512-67781165, zongping_luo@yahoo.com.

Authors' Contributions

Xi Chen, Fan He, and Zong-Ping Luo conceived and designed the study. Xi Chen and Jinku Yan performed experiments and analyzed the data. Dongyan Zhong assisted in assembling the mechanical loading device. Xi Chen and Fan He wrote the manuscript. Huilin Yang, Ming Pei, and Zong-Ping Luo contributed to writing and revising the manuscript. Fan He and Zong-Ping Luo supervised all phases of the project. All authors reviewed the manuscript and have approved the final version for submission.

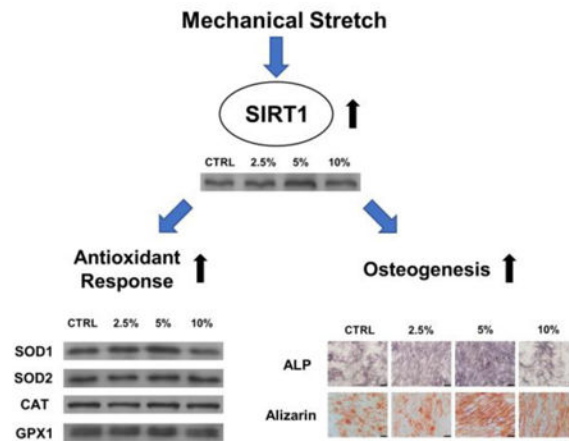
Conflicts of Interest

The authors declare no conflicts of interest.

Publisher's Disclaimer: This is a PDF file of an unedited manuscript that has been accepted for publication. As a service to our customers we are providing this early version of the manuscript. The manuscript will undergo copyediting, typesetting, and review of the resulting proof before it is published in its final citable form. Please note that during the production process errors may be discovered which could affect the content, and all legal disclaimers that apply to the journal pertain.

especially superoxide dismutase 1 (SOD1), were up-regulated. Osteogenesis was improved by 5% stretch rather than 10% stretch, as evidenced by increased matrix mineralization and osteogenic marker gene expression. The expression of SIRT1 and phosphorylation of AMPK were enhanced by mechanical stretch; however, inhibition of SIRT1 or AMPK abrogated the stretch-induced antioxidant effect on BM-MSCs and inhibited the stretch-mediated osteogenic differentiation. Our findings reveal that mechanical stretch induced antioxidant responses, attenuated intracellular ROS, and improved osteogenesis of BM-MSCs. The stretch-induced antioxidant effect was through activation of the AMPK-SIRT1 signaling pathway. Our findings demonstrated that appropriate mechanical stimulation can improve MSC antioxidant functions and benefit bone regeneration.

Graphical Abstract:



Keywords

mesenchymal stem cells; cyclic stretch; SIRT1; AMPK; superoxide dismutase; osteogenesis

Introduction

Mesenchymal stem cells (MSCs) have attracted great attention in regenerative medicine and tissue engineering because of their accessibility, robust self-renewal capacity, and multi-differentiation potential. Increasing evidence indicates that mechanical forces, such as stretch, tension, compression, and fluid shear stress, play a critical role in regulating MSC behavior and their functions [1]. For example, mechanical loading from physical activities has been proven to be beneficial to bone mineral density and bone strength, because bone marrow-derived mesenchymal stem cells (BM-MSCs) can translate external mechanical stimuli into intracellular biochemical signals. These signals can promote differentiation toward the osteoblast lineage and synthesis of new bone matrix [2]. In contrast, dysregulation of mechanical loading, such as osteoporosis during immobilization or during long-duration space flight, may lead to bone diseases [3].

Reactive oxygen species (ROS), such as the superoxide anion radical (O_2^-), hydrogen peroxide (H_2O_2), and the hydroxyl radical (HO^\cdot), have been suggested to play an important

role in mechanosensitive signaling transduction [4]. In response to mechanical stimuli, these species are mainly generated in a cell membrane-associated NADPH oxidase [5] and the mitochondrial electron transport chain contributes to stretch-induced ROS generation as well [6]. A growing body of evidence has demonstrated that physiological levels of ROS, as a secondary messenger, are crucial to the self-renewal and multi-lineage differentiation of stem cells [7]. Schmelter et al. showed that intracellular ROS were involved in mechanical strain-induced cardiovascular differentiation of embryonic stem cells through activation of the extracellular-regulated kinase 1/2 (ERK1/2) signaling cascade [8]. However, excessive levels of ROS have been proven to cause oxidative stress in MSCs, leading to lipid and protein oxidation, DNA damage, premature senescence, or cell death [9]. A recent study showed that chronic exposure of human pulmonary endothelial cells to a pathological level of cyclic stretch (at 18% magnitude) induced an inflammatory response, while treatment with antioxidant *N*-acetyl cysteine (NAC) attenuated ROS accumulation and ameliorated stretch-induced inflammation [10].

Apart from the production of ROS, redox homeostasis in cells is influenced by intracellular antioxidant enzymes, including superoxide dismutase (SOD), catalase (CAT), glutathione peroxidase (GPx), peroxiredoxin, and glutaredoxin. These enzymes convert cytotoxic ROS into nontoxic metabolites such as oxygen and water. For example, SOD1 is predominantly located in cytoplasm and nucleus, while SOD2 is found in the mitochondrial matrix. Both of them can catalyze O_2^- to H_2O_2 , which can be neutralized to water by catalase and GPx [11]. In response to mechanical loading such as exercise, the intracellular antioxidant defense has been reported to increase in skeletal muscle cells [12]. Morikawa and colleagues demonstrated that loss of SOD1 exacerbated bone loss and they suggested activation of SOD1 would be a promising strategy for preventing bone loss [13].

Silent information regulator type 1 (SIRT1), a member of nicotinamide adenine dinucleotide (NAD⁺)-dependent deacetylases, has been shown to regulate metabolism, cell growth, differentiation, and antioxidant responses in MSCs. Activation of SIRT1 by resveratrol (ResV) has been shown to improve mitochondrial SOD2 function in diabetic mice [14]. Meanwhile, SIRT1 is crucial for preventing cellular senescence by delaying the accumulation of p16^{INK4a} (an important cell cycle inhibitor) and thus contributes to the long-term growth of human MSCs [15]. SIRT1 has also been suggested to play an essential role in maintaining the multi-differentiation potentials of BM-MSCs through deacetylation of SRY (sex determining region Y)-box 2 (SOX2) [16]. Previous studies from our laboratory revealed that activation of SIRT1 protected MSCs from oxidative stress-induced premature senescence [17] and rescued alcohol-inhibited osteogenic differentiation in BM-MSCs [18]. Recently, Pardo et al. showed that mechanical stretch resulted in an increase in ROS generation and up-regulated the levels of SIRT1 in skeletal muscle cells. Further molecular experiments suggested that SIRT1 was involved in protecting against stretch-induced oxidative stress through the early growth response factor 1 (EGR)-dependent signaling pathway [19]. However, the underlying mechanisms by which mechanical signals regulate antioxidant functions of MSCs and whether this response is mediated by the SIRT1-dependent mechanosensitive signaling pathways are not fully understood.

In the present study, human BM-MSCs were exposed to mechanical stretch at different strain magnitudes of 2.5%, 5%, and 10%. We analyzed the effect of mechanical stretch on global gene expression profile and antioxidant changes in BM-MSCs, such as SOD1, SOD2, CAT, and GPx1. The effect of cyclic stretch on cell proliferation, intracellular ROS, and osteogenesis were also evaluated. Moreover, we investigated the molecular mechanisms involved the AMP-activated protein kinase (AMPK) and SIRT1 signaling pathways.

Materials and Methods

Reagents and antibodies

Human BM-MSCs were purchased from Cyagen Biosciences Inc. (Guangzhou, China). Fetal bovine serum (FBS), alpha minimum essential medium (α -MEM), penicillin, streptomycin, TRIzol[®] reagent, Dulbecco's modified Eagle medium (DMEM), trypsin-ethylene diamine tetraacetic acid (EDTA), horseradish peroxidase-conjugated secondary antibodies, protease inhibitor tablets, and SuperSignal West Pico Substrate were purchased from Thermo Fisher Scientific (Waltham, MA, USA). Standard cell culture plates and flasks were purchased from Costar (Tewksbury, MA, USA). Fibronectin, 2',7'-dichlorofluorescein diacetate (DCFH-DA), 4',6-diamidino-2-phenylindole (DAPI), paraformaldehyde, L-ascorbic acid, dexamethasone, β -glycerol phosphate, Sirtinol, Compound C (CC), and phosphate buffered saline (PBS) were obtained from Sigma-Aldrich (St. Louis, MO, USA). Primary antibodies against SOD1, SOD2, CAT, GPx1, SIRT1, AMPK, p-AMPK (phospho T183 + T172), and glyceraldehyde-3-phosphate dehydrogenase (GAPDH) were purchased from Abcam (Cambridge, MA, USA). Cell lysis buffer, polyacrylamide gels, nitrocellulose membranes, and X-OMAT BT Film were purchased from Beyotime Institute of Biotechnology (Haimen, China). All other materials and reagents were purchased from diverse conventional suppliers.

Cell culture

Human BM-MSCs (passage 1) were cultured in growth medium containing α -MEM, 10% FBS, 100 U/mL of penicillin, and 100 μ g/mL of streptomycin at 37°C with 5% CO₂. The medium was changed every three days. BM-MSCs were cultured two more passages to obtain a sufficient amount and these cells (passage 4) were used in the experiments as described below.

Application of cyclic stretch to BM-MSCs

The mechanical stretch device consisted of a computer system, a control unit, a driving motor, and cell culture silicone chambers (3 cm \times 6 cm) (Suppl Fig. 1A). The substrate of the cell culture chambers was made with SYLGARD[®] 184 (Dow Corning GmbH, Wiesbaden, Germany) and, after sterilization, the silicone substrate was coated with fibronectin (1 μ g/cm²) at 37°C for 2 h. BM-MSCs were plated on the pre-treated silicone membrane at an initial density of 3,000 cells/cm². After 24 h, the cells were subjected to longitudinal stretch that was produced by the computer-controlled device and the following mechanical parameters were applied: frequency of 1 Hz, linear magnitude of 2.5%, 5%, or 10%, and duration of 2 h per day (Suppl Fig. 1B&C). During cyclic stretch, cells were

maintained in an incubator at 37°C with 5% CO₂. Cells cultured under static conditions served as the control group (CTRL).

Treatments with CC or Sirtinol

To investigate the role of AMPK in response to mechanical stretch, BM-MSCs were pre-incubated with 10 μM CC (an AMPK inhibitor) for 2 h and then subjected to 5% cyclic stretch for 3 days (2 h per day). To investigate the role of SIRT1 in mediating the antioxidant responses to mechanical stretch, BM-MSCs were pre-incubated with 40 μM Sirtinol (a SIRT1 inhibitor) for 2 h and then subjected to 5% cyclic stretch for 3 days (2 h per day).

Immunofluorescence staining of F-actin

After a 3-day cyclic stretch, BM-MSCs were fixed in 4% paraformaldehyde for 10 min. After treating with 0.1% Triton X-100 in PBS for 5 min, cells were incubated in rhodamine phalloidin staining solution (MesGen Biotech, Shanghai, China) at room temperature for 40 min following the manufacturer's protocol. Cell nuclei were counterstained with DAPI. Immunofluorescence images of F-actin were visualized and captured using a Zeiss Axiovert 40CFL microscope (Zeiss, Oberkochen, Germany).

Cell proliferation

A Cell Counting Kit-8 assay (CCK-8; Beyotime) was performed to evaluate cell proliferation as described previously [17]. Briefly, BM-MSCs were seeded on pre-treated silicone membranes at a density of 1,000 cells/cm². Cells were subjected to cyclic stretch (2.5%, 5%, and 10%) for 2 h per day. At days 1, 3, 5, and 7, the CCK-8 solution was added in each chamber and the cells were incubated at 37°C for 1 h. The absorbance was measured at 450 nm using a microplate spectrophotometer (BioTek, Winooski, VT, USA). The absorbance values were normalized to the value of day 1.

Microarray for gene expression analysis

Gene expression profiles were assessed by the Affymetrix Human HTA2.0 expression microarrays (Affymetrix, Santa Clara, CA, USA). BM-MSCs were plated at confluence on pre-treated silicone membranes and subjected to 5% cyclic stretch for 3 days (2 h per day). Total RNA was extracted using TRIzol[®] reagent according to the manufacturer's protocol and quantified by the NanoDrop ND-2000 (Thermo Scientific). The RNA integrity was assessed using Agilent Bioanalyzer 2100 (Agilent Technologies, Santa Clara, CA, USA). The microarray experiments were performed at Shanghai OE Biotech. Co., Ltd. (Shanghai, China). The gene expression levels between the CTRL group and the stretch group were compared using the Significant Analysis of Microarray software (SAM) and enrichment analyses for the Gene Ontology (GO) biological process were performed using WebGestalt. The differentially expressed genes were identified by a fold-value change of ≥ 1.5 in the SAM output results.

Intracellular ROS detection

Measurement of intracellular ROS in BM-MSCs was performed as described previously [20]. After 3 days of cyclic stretch, cells were dissociated by 0.25% trypsin-EDTA and then

incubated in 10 μ M of DCFH-DA solution at 37°C for 10 min. After washing twice with PBS, the fluorescence intensity was measured using a Guava easycyte Flow Cytometer (Millipore, Boston, MA, USA) and 20,000 events from each cell sample were analyzed using the FlowJo 7.6.1 software (TreeStar, San Carlos, CA, USA). Unstained cells were applied as background and the levels of ROS were normalized to the control group.

SOD activity assay

Total SOD activity was analyzed using a commercially available SOD assay kit (Beyotime) according to the manufacturer's instructions. After 3 days of stretch, BM-MSCs were suspended in cell lysis solution and protein amount was quantified with the BCA protein assay kit (Beyotime). Each lysate was mixed with reagent from the kit and incubated at 37°C for 20 min. Absorbance at 450 nm was measured using a microplate reader (BioTek).

Osteogenic differentiation of BM-MSCs

To investigate the effect of mechanical stretch on osteogenic differentiation, BM-MSCs were induced toward osteogenic differentiation. Cells were incubated in osteogenic medium, in which the DMEM was supplemented with 10% FBS, 10 mM β -glycerol phosphate, 100 nM dexamethasone, and 50 μ g/mL L-ascorbic acid. Cyclic stretch at magnitudes of 2.5%, 5%, and 10% was applied for 2 h per day. Cells cultured under static conditions were used as the control group (CTRL). Osteogenic medium was refreshed every 3 days.

To explore the underlying mechanisms in stretch-mediated osteogenesis, BM-MSCs were incubated in osteogenic medium supplemented with 10 μ M CC or 40 μ M Sirtinol. The cells were subjected to 5% cyclic stretch for 14 days (2 h per day). Cells cultured under static conditions were used as the control group (CTRL).

Alkaline phosphatase (ALP) staining and activity measurement

After a 7-day osteogenic induction, ALP activity was measured using commercially available kits. To qualitatively observe ALP-positive cells, BM-MSCs were washed three times with PBS, fixed with 4% paraformaldehyde, and stained with a BCIP/NBT Alkaline Phosphatase Color Development Kit (Beyotime) for 15 min according to the manufacturer's instructions. Digital images were captured using an Olympus IX51 microscope (Olympus Corporation, Tokyo, Japan).

To quantitatively measure ALP activity, BM-MSCs were dissolved in ice-cold cell lysis buffer and, after centrifuging, the supernatant was divided into two parts. One part was evaluated colorimetrically using an ALP Assay Kit (Beyotime) according to the manufacturer's protocol. The other part was used to determine protein concentrations using a BCA protein assay kit (Beyotime). The ALP activity was normalized to the total protein content.

Evaluation of matrix mineralization using Alizarin Red S staining

After a 14-day osteogenic induction, BM-MSCs were fixed in 4% paraformaldehyde and incubated in 1% Alizarin Red S solution (pH = 4.3; Sigma-Aldrich) at room temperature for 15 min. After washing twice with PBS, digital images were captured using an Olympus

IX51 microscope. To quantify the level of matrix mineralization, two hundred microliters of hydrochloric acid (1%;Sigma-Aldrich) was added to each chamber to dissolve the stain from calcified layers. The absorbance was measured at 420 nm using a microplate spectrophotometer and the values were normalized to the control group.

Reverse transcription-quantitative polymerase chain reaction (RT-qPCR)

Total RNA was extracted from BM-MSCs using TRIzol[®] reagent and then reverse-transcribed to cDNA using the RevertAid First Strand cDNA Synthesis Kit (Thermo Fisher) according to the manufacturer's instructions. Quantitative PCR was performed using the iTap[™] Universal SYBR[®] Green Supermix kit (Bio-Rad, Hercules, CA, USA) on a CFX96[™] Real-Time PCR System (Bio-Rad) following the manufacturer's protocol. Transcript levels of *SIRT1* and antioxidant enzymes, including *CAT*, *GPX1*, *SOD1*, and *SOD2*, were evaluated. Osteogenic marker genes, including *ALP*, *BGLAP* (bone gamma carboxyglutamate protein), *RUNX2* (runt-related transcription factor 2), and *SP7* (osterix) were also evaluated. Primer sequences for target genes are listed in Table 1, with *GAPDH* as an internal standard. Relative transcript levels of target genes were calculated as described previously [21].

Western blot analysis

After 3 days of stretch, BM-MSCs were incubated in lysis buffer containing protease inhibitors for 1 h on ice. Protein concentrations were quantified using a BCA protein assay kit (Beyotime). Equal amounts of protein from each extract were denatured and separated in a 10% polyacrylamide gel, and then transferred by electrophoresis onto a nitrocellulose membrane. Membranes were blocked in blocking buffer (Beyotime) for 30 min and incubated in properly diluted primary antibodies at 4°C overnight. The membranes were incubated in respective horseradish peroxidase-conjugated secondary antibodies at room temperature for 1 h and then developed using SuperSignal West Pico Substrate and X-OMAT BT Film. The intensity of bands was quantified using ImageJ software (National Institutes of Health, Bethesda, MD, USA).

Statistical analysis

Statistical analysis was conducted using the SPSS 13.0 statistical software (SPSS Inc., Chicago, IL, USA). All data were expressed as means \pm standard error of mean (S.E.M.). Statistical differences were determined using the two-tailed Student's *t*-test for comparisons between two groups and one-way Analysis of Variance (ANOVA) with a Tukey's post hoc test for multiple group comparisons. Statistically significant differences are indicated by * where $p < 0.05$ between the indicated groups and # where $p < 0.05$ vs. the CTRL group.

Results

Effects of mechanical stretch on cell morphology and proliferation of BM-MSCs

BM-MSCs were exposed to mechanical cyclic stretch for 2 h per day at the magnitudes of 2.5%, 5%, and 10% and, after 3 days of stretch, the cell cytoskeleton F-actin was stained by rhodamine phalloidin. BM-MSCs under static conditions showed a flattened and polygonal cell shape, but the morphology of stretch-treated cells became slender and spindle-like. We

also observed that BM-MSCs in the stretch groups grew along the direction of longitudinal mechanical force, in contrast to random migration directions of cells in the CTRL group (Fig. 1A). The effect of mechanical stretch on cell proliferation was assessed at days 1, 3, 5, and 7. On day 7, BM-MSCs in the 5% stretch group yielded the highest level of cell proliferation (14.9% higher than the CTRL group, 13.2% higher than the 2.5% stretch group, and 16.5% higher than the 10% stretch group) (Fig. 1B).

Global gene expression analysis of stretch-treated BM-MSCs

To examine changes in gene expression caused by mechanical stretch, microarray analyses were performed using total RNA extracted from BM-MSCs in the CTRL group and the 5% stretch group. The heat map showed an overview of differentially expressed genes that were defined as the 1.5-fold up- or down-regulated genes (Fig. 2A). A total of 793 differentially expressed genes were identified in BM-MSCs subjected to 5% stretch, in comparison to cells cultured under static conditions. Among these, 275 genes were up-regulated, including 83 genes encoding well-defined proteins (Suppl Table 1), while 518 genes were down-regulated, including 159 genes encoding well-defined proteins (Suppl Table 2). We then performed functional enrichment analysis of biological processes. The top fifteen biological processes up- or down-regulated by stretch stimulation were shown in Fig. 2B&C. Among these, extracellular matrix organization, bone mineralization, and collagen fibril organization were up-regulated, while the processes of extracellular matrix disassembly, cellular response to zinc ion, and cellular response to fluid shear stress were down-regulated in the stretch group.

Mechanical stretch induces antioxidant responses in BM-MSCs

We evaluated the levels of two important antioxidant enzymes, SOD1 and SOD2, which scavenge intracellular superoxide radicals. In comparison with the CTRL group, treatments with mechanical stretch significantly increased the transcript levels of *SOD1* by 28.6% at 2.5% magnitude and 95.8% at 5% magnitude; however, the expression of SOD1 was suppressed by treatment with 10% stretch (Fig. 3A). Similarly, treatments with mechanical stretch significantly increased the transcript levels of *SOD2* by 19.3% at 2.5% magnitude and 26.4% at 5% magnitude (Fig. 3B). In addition, the levels of SOD activity were enhanced by treatment with mechanical stretch (by 34.0% at 2.5% magnitude and 54.8% at 5% magnitude) (Fig. 3C). Consistently, the western blot assay confirmed that the protein levels of SOD1 were up-regulated by treatments with mechanical stretch (Fig. 3D). Quantitative analysis showed that treatment with 5% stretch increased the SOD1 level by 54.1% (Suppl Fig. 2A), but the differences of SOD2 expression between the CTRL and stretch groups were not significant (Suppl Fig. 2B).

In addition, we investigated the effect of mechanical cyclic stretch on intracellular H₂O₂ scavenging enzymes, CAT and GPx1. The mRNA level of *CAT* was up-regulated by 13.5% in the 5% stretch group compared with the CTRL group (Fig. 3E). Treatments with mechanical stretch significantly increased the transcript levels of *GPX1* by 19.4% at 2.5% magnitude and 37.0% at 5% magnitude, compared with the static cells (Fig. 3F). The protein levels of CAT and GPx1 were determined using western blot assays (Fig. 3G). Quantitative analysis showed that the protein levels of CAT in all groups were not significantly different

(Suppl Fig. 2C), but treatment with 5% stretch significantly up-regulated the protein expression of GPx1 by 68.6% compared with the static cells (Suppl Fig. 2D).

Mechanical stretch increases SIRT1 expression and AMPK phosphorylation

After being subjected to mechanical cyclic stretch for 3 days, the levels of intracellular ROS in BM-MSCs were determined by flow cytometry (Fig. 4A). The results showed that treatments with mechanical stretch significantly decreased the levels of ROS by 21.2% at 2.5% magnitude and 39.2% at 5% magnitude, compared with the static cells; however, 10% stretch showed no effect on the generation of ROS in BM-MSCs (Fig. 4B). Since SIRT1 plays an important role in modulating the intracellular antioxidant system, we evaluated both the mRNA and protein expression of SIRT1. RT-qPCR data showed that, compared with the CTRL group, the transcript level of *SIRT1* was significantly up-regulated by mechanical cyclic stretch (by 78.6% at 2.5% magnitude, 315.5% at 5% magnitude, and 17.0% at 10% magnitude) (Fig. 4C). The western blot assay showed that treatment with 5% stretch significantly increased the protein level of SIRT1 by 46.4% compared with the CTRL group (Fig. 4D&E). In addition, the involvement of the AMPK signaling pathway was determined (Fig. 4F). The results showed that treatments with mechanical stretch significantly enhanced the phosphorylation levels of AMPK by 26.4% at 2.5% magnitude and 53.8% at 5% magnitude, compared with the static cells (Fig. 4G), while the total expression of AMPK was similar in all groups (Fig. 4H).

Mechanical stretch promotes osteogenic differentiation of BM-MSCs

The effect of mechanical cyclic stretch on osteogenic differentiation was assessed. BM-MSCs were induced toward an osteogenic lineage commitment and, after a 7-day induction, the levels of ALP (a typical marker for early osteogenesis) activity were determined. The ALP staining assay showed more positively-stained cells in the 2.5% stretch and 5% stretch groups than in the CTRL group (Fig. 5A). Quantitative analysis revealed that mechanical stretch increased ALP activity in BM-MSCs by 76.5% at 2.5% magnitude and 124.5% at 5% magnitude, compared with the static cells (Fig. 5B); however, the level of ALP activity in the 10% stretch group was 16.6% lower than the CTRL group ($p = 0.19$). The transcript levels of *ALP* were up-regulated by mechanical stretch (by 30.6% at 2.5% magnitude and 77.8% at 5% magnitude) (Fig. 5C). Furthermore, Alizarin Red S staining was used to determine matrix mineralization (a typical marker for the late stage of osteogenesis) and, after a 14-day induction, differentiated BM-MSCs in the 5% stretch group showed the strongest staining (Fig. 5D). The quantitative results demonstrated that the level of calcium deposition was 20.9% higher in the 5% stretch group than the CTRL group (Fig. 5E). RT-qPCR data confirmed that mechanical stretch significantly increased the transcript levels of osteoblast-specific markers. The mRNA expression of *BGLAP* was up-regulated by 28.1% and 80.4% in the 2.5% and 5% stretch groups, respectively (Fig. 5F). Cyclic stretch of 5% magnitude significantly increased the gene expression of *RUNX2* (Fig. 5G) and *SP7* (Fig. 5H) by 1.4-fold and 60.0%, respectively.

Inhibition of SIRT1 abrogates mechanical stretch-induced antioxidant effects on BM-MSCs

To confirm the involvement of the AMPK-SIRT1 signaling pathway in modulating mechanical stretch-induced antioxidant effects, BM-MSCs were pre-treated with 10 μ M CC

to inhibit AMPK activation or 40 μ M Sirtinol to suppress SIRT1 activity. The western blot assay showed that the phosphorylation of AMPK was significantly decreased by pre-treatment with CC (Fig. 6A). The phosphorylated levels of AMPK were 39.6% and 55.6% lower than the static cells and the stretch-treated cells, respectively (Fig. 6B), while the total expression of AMPK protein was not affected by the CC pre-treatment (Fig. 6C). RT-qPCR data showed that Sirtinol treatment significantly decreased the transcript levels of *SIRT1* by 32.9% in static conditions and by 73.2% in 5% stretch treated BM-MSCs (Fig. 6D). In static conditions, Sirtinol treatment did not affect the protein expression of SIRT1, but it significantly down-regulated the SIRT1 level in 5% stretch treated BM-MSCs (by 18.2% compared with the 5% stretch group) (Fig. 6E&F).

Furthermore, we examined whether inhibition of AMPK or SIRT1 would counteract the mechanical stretch-induced antioxidant effects on BM-MSCs. When subjected to 5% cyclic stretch, treatment with CC and Sirtinol decreased the transcript levels of *SOD1* by 44.1% and 55.9%, respectively (Fig. 7A). In stretch-treated BM-MSCs, treatments with CC and Sirtinol down-regulated the mRNA expression of *SOD2* by 19.0% and 40.9%, respectively (Fig. 7B). Western blot assay demonstrated that the protein levels of SOD1 and SOD2 were also down-regulated by treatment with or Sirtinol (Fig. 7C). Compared to the stretch group, Sirtinol treatment significantly down-regulated the protein level of SOD1 by 39.9% (Suppl Fig. 3A) and the expression of SOD2 by 39.4% (Suppl Fig. 3B). With regard to H₂O₂ scavenging enzymes, treatment with Sirtinol decreased the mRNA level of *CAT* by 41.2% (Fig. 7D) and the expression of *GPX1* by 48.2% (Fig. 7E). The effects of treatment with CC and Sirtinol on the protein levels of CAT and GPx1 was confirmed by the western blot experiments (Fig. 7F). Compared to the stretch group, Sirtinol treatment down-regulated the protein level of CAT by 33.1% (Suppl Fig. 3C) and the expression of GPx1 by 49.3% (Suppl Fig. 3D).

Inhibition of AMPK or SIRT1 suppressed the osteogenic differentiation of stretch-treated BM-MSCs

To further explore the role of SIRT1 in regulating stretch-mediated osteogenesis, BM-MSCs were treated with 10 μ M CC or 40 μ M Sirtinol to inhibit AMPK or SIRT1 activities. After a 14-day induction, the results of Alizarin Red S staining showed that treatments with CC or Sirtinol suppressed calcium deposition in BM-MSCs (Fig. 8A). The quantitative data confirmed that, when subjected to 5% cyclic stretch, treatment with CC and Sirtinol decreased the levels of matrix mineralization by 37.4% and 71.1%, respectively (Fig. 8B). RT-qPCR data showed that, in stretch-treated BM-MSCs, treatments with CC and Sirtinol down-regulated the mRNA expression of *BGLAP* by 58.1% and 71.1%, respectively (Fig. 8C). Compared to the stretch group, Sirtinol treatment significantly decreased the transcript level of *RUNX2* by 76.5% (Fig. 8D) and the gene expression of *SP7* by 55.8% (Fig. 8E).

Discussion

Mechanical loading plays an important role in regulating skeletal tissue homeostasis; thus, a number of studies have been conducted to investigate the effects of mechanical stimulation on skeletal cells, including osteoblasts, chondrocytes, skeletal muscle cells, and endothelial

cells. It has been shown previously that cell proliferation of human tendon cells [22], as well as venous smooth muscle cells [23], was improved by cyclic stretch. In this study, we treated cells with longitudinal stretch with 2.5% and 5% magnitude to mimic physiological loading and found that appropriate mechanical stimulation increased cell proliferation of BM-MSCs. On the other hand, we chose to use 10% mechanical strain to mimic pathological stretch and showed that cell growth was barely affected, suggesting that only mechanical stimulation at physiological levels had a positive effect on cell proliferation. Mechanical stretch with overloaded magnitudes, such as 20% elongation [24], was reported to induce apoptosis of alveolar epithelial cells. Tan and colleagues demonstrated that excessive levels of cyclic stretch resulted in cell death in myoblast C2C12 cells through generation of abundant ROS and activation of c-Jun NH2-terminal kinase 1 (JNK1) [25]. As well, excessive mechanical loading was found to promote inflammatory responses by up-regulating the expression of Toll-like receptors (TLRs) and tumor necrosis factor α (TNF α) in human intervertebral disc cells, eventually leading to spinal disc degeneration and low-back pain [26]. Further molecular experiments revealed that mechanical stretch-induced endoplasmic reticulum (ER) stress may also be responsible for increased apoptosis, inflammation, and degeneration [27].

ROS formation in response to mechanical stimulation has been demonstrated in previous studies. Exposure of vascular smooth muscle cells to cyclic mechanical stretch resulted in a rapid ROS generation in a NADPH oxidase-dependent manner [28]. Dick and colleagues further investigated the mechanisms involving stretch-induced ROS generation and demonstrated that cyclic stretch increased intracellular H₂O₂, nitric oxide, and peroxynitrite in pulmonary arterial smooth muscle cells [29]. However, in this study, we observed a decrease in intracellular ROS after BM-MSCs were subjected to 2.5% and 5% cyclic stretch. We speculate that the disagreement in ROS levels was caused by the experimental time points. In previous studies, ROS formation was determined immediately after mechanical loading; however, in this study, the ROS levels were measured after a 3-day cyclic stretch (2 h per day). It is possible that ROS levels were transiently increased by mechanical stretch in the beginning stage but declined due to stretch-induced antioxidant responses. Pardo et al. demonstrated that the maximal level of superoxide production was achieved 1 h after stretch and then progressively decreased to a basal level in skeletal muscle cells [19]. Therefore, the mechanical stretch-induced antioxidant responses might be responsible for attenuation of ROS levels.

In this study, we evaluated the inductive effect of mechanical stretch on the expression of intracellular antioxidant enzymes, such as SOD1, SOD2, CAT, and GPx1. Our results showed both the expression and activity of SOD in BM-MSCs were up-regulated by cyclic stretch at 2.5% and 5% magnitudes. In agreement with our results, it has been reported that cyclic strain stimulated the induction of antioxidant and detoxifying enzymes in human dental pulp cells, such as SOD1, GPx1, and heme oxygenase-1 (HO-1) [30]. Activation of the defense antioxidant system represented a compensatory adaptation in response to mechanical stress, which might mediate a protective effect on cells against stress-induced oxidative stress or tissue injuries. Without the protection of antioxidant enzymes, the beneficial effect of mechanical loading, such as exercise, would be lost and could even cause serious tissue damage or degenerative diseases. Pate and colleagues conducted a study in

which transgenic mice with reduced levels of extracellular SOD (SOD3) were exposed to running on a treadmill. The transgenic mice showed significant damage to cartilage tissue and lower levels of bone strength compared with wild-type mice and they demonstrated that loss of SOD3 might account for stress-induced osteoarthritis [31]. More importantly, we found that the levels of antioxidant enzymes in BM-MSCs were decreased by 10% cyclic stretch in this study. In agreement with our results, Li et al. reported that excessive mechanical strain (from 12% to 24% magnitude) resulted in a significant decrease in the activity of SOD but an increase in ROS generation in a magnitude-dependent manner[32]. Therefore, mechanical stimulation at an appropriate and physiologic magnitude can benefit cell functions by protecting cells from oxidative damage, but excessive or pathologic stretch had an adverse effect on cells.

Furthermore, our results demonstrated that SOD1 rather than SOD2 was selectively up-regulated in BM-MSCs in response to mechanical stretch, suggesting that SOD1 was more sensitive to mechanical stimulation. Different from undifferentiated BM-MSCs, it has been reported that the expression of SOD2 was increased by mechanical stretch in C2C12 myoblasts [19] and by treadmill running in rat skeletal muscle tissues [33]. In human cartilage chondrocytes, mechanical overloading resulted in selective SOD2 down-regulation and subsequently an increase in mitochondrial superoxide generation [34]. However, the mechanisms underlying the different expression of SOD1 and SOD2 in response to mechanical loading are not fully understood. One explanation is that the energy metabolism of undifferentiated MSCs and differentiated cells (e.g., osteoblasts) is different. A recent study from our laboratory demonstrated a time-dependent up-regulation of both SOD1 and SOD2 upon the osteogenic induction of BM-MSCs, but the levels of SOD2 rather than SOD1 showed larger differences in late-differentiated osteoblasts compared with undifferentiated MSCs [35]. In the future, the effects of mechanical stretch on the intracellular antioxidant defense system of differentiated osteoblasts or osteocytes will be further investigated.

An important finding of our present study is that SIRT1 is identified as a crucial mechanosensitive factor, which regulates the antioxidant defense in stretch-treated BM-MSCs. Both mRNA and protein expression of SIRT1 were up-regulated in BM-MSCs during cyclic stretch treatment, in accordance with the increased levels of intracellular antioxidant enzymes. Blockage of SIRT1 activity by Sirtinol abrogated the stimulatory effect of mechanical stretch on antioxidant enzyme expression. In agreement with our results, a previous study reported that SIRT1 was activated by mechanical stress in human periodontal ligament cells [36] in a force- and time-dependent manner. In addition, our results indicated that mechanical stretch-induced up-regulation of SIRT1 was through activation of AMPK, because inhibition of AMPK by CC significantly reduced the expression of SIRT1 and down-regulated the levels of antioxidant enzymes. Kim et al. showed that resveratrol prevented high-glucose-induced oxidative stress and apoptosis in the kidneys of diabetic mice through activation of the AMPK-SIRT1 signaling pathway [37]. The regulation of antioxidant enzyme expression by SIRT1 depended on its deacetylation activity on the transcription factor Forkhead box type O transcription factor 3a (FoxO3a) and the transcriptional coactivator peroxisome proliferator activated receptor γ -coactivator 1 α (PGC-1 α) [38]. SIRT1 promoted the nuclear translocation of FoxO3a and thus induced the

transcription of antioxidant enzymes, such as SOD2 and CAT [39]. As well, the Nrf2 (nuclear factor-E2 related factor 2)/ARE (antioxidant response element) signaling pathway was possibly involved in the molecular mechanisms in terms of SIRT1-mediated antioxidant protection from oxidative stress [40]. Therefore, further investigations are necessary to explore the role of SIRT1 and the subsequent signaling pathways in the stretch-induced antioxidant responses in BM-MSCs.

Mechanical loading has been proven to regulate the osteogenic differentiation of MSCs and, in the present study, we showed that cyclic stretch at 2.5% and 5% magnitude improved osteogenesis in BM-MSCs, as evidenced by enhanced matrix mineralization and increased gene expression of osteogenic markers. Analysis of the global gene expression revealed that mechanical stretch regulated biological processes associated with osteogenic differentiation. For example, exposure of MSCs to cyclic stretch resulted in up-regulation of anabolic processes, such as extracellular matrix (ECM) organization, bone mineralization, and collagen fibril organization. On the other hand, several catabolic processes were down-regulated, including ECM disassembly and proteolysis. These results indicated that mechanical stretch facilitated osteogenesis of BM-MSCs by promoting ECM synthesis. In addition, stretch-induced activation of SIRT1 might contribute to enhanced osteogenic differentiation. SIRT1 promoted the lineage commitment of MSCs to osteogenesis by enhancing the transcriptional activity of FoxO3a and up-regulating the expression of RUNX2, which was critical in regulating transcription of downstream osteoblast-specific marker genes [41]. Inhibition of SIRT1 using Sirtinol or silencing its gene expression by RNA interference suppressed osteogenesis of human periodontal ligament cells [42]. Consistently, our results confirmed that inhibition of SIRT1 by Sirtinol treatment significantly suppressed stretch-induced osteogenesis. Apart from the direct stimulatory effect, the SIRT-mediated antioxidant effect could benefit the maturation of BM-MSCs toward osteoblasts. Recently, we reported that the SIRT1 signaling pathway was actively involved in MSC osteogenesis. A positive relationship between SIRT1 and intracellular antioxidant enzymes was observed, which accounted for the enhanced resistance to oxidative stress upon osteogenic differentiation [43]. In addition, Ho et al. observed elevated levels of intracellular H₂O₂ in long-term cultured human MSCs that were responsible for the decline of osteogenic differentiation capacity. Scavenging of H₂O₂ using NAC restored the osteogenic capacity of senescent MSCs by increasing the expression of V-maf musculoaponeurotic fibrosarcoma oncogene homolog (c-MAF), which is an osteogenic and age-sensitive transcription factor [44]. Choi et al. used an intracellular delivery system with a cell-penetrating peptide to successfully deliver SOD1 into human dental pulp stem cells and it was shown effective for reversing the inhibition of osteoblastic differentiation and down-regulation of osteogenic gene markers induced by H₂O₂ [45].

However, the beneficial effects of mechanical stimulation on osteogenesis is dependent on the stretch magnitude. We found that exposure of BM-MSCs to 10% stretch showed no effect on osteogenic differentiation. Compared with the 5% stretch group, the activity and expression of ALP in BM-MSCs subjected to 10% stretch were significantly lower, suggesting that excessive stretch might have an adverse effect on cell differentiation. In addition, the types of mechanical strain application are important to affect stem cell behavior and functions. Different from the intermittent stretch loading that stimulated BM-MSCs for

2 h every day in this study, continuous cyclic mechanical tension showed inhibitory effects on the expression of osteogenic genes such as RUNX2 in human BM-MSCs [46]. Furthermore, age is another essential factor for regulating MSC functions in response to mechanical loading. Tan et al. showed that cyclic stretch resulted in significantly decreased osteogenesis in MSCs from adult rats, but enhanced osteogenesis in MSCs from young rats. The compromised osteogenesis in aged MSCs was caused by stretch-induced ROS overproduction and reduced SOD1 activity [47].

Conclusions

In summary, we demonstrated that cyclic stretch induced antioxidant responses and improved the osteogenic differentiation of human BM-MSCs. The stretch-induced up-regulation of intracellular antioxidant enzymes, especially SOD1 in BM-MSCs, was through activation of the AMPK-SIRT1 signaling pathway. Our findings uncovered a critical role of SIRT1 as a mechanosensitive factor in regulating intracellular ROS and the antioxidant defense system in response to mechanical stimulation. We also showed that the enhanced antioxidant functions and osteogenic differentiation of BM-MSCs were counteracted by excessive mechanical stretch. Taken together, our findings indicate that appropriate mechanical stimulation can maintain redox balance and benefit bone regeneration.

Supplementary Material

Refer to Web version on PubMed Central for supplementary material.

Acknowledgments

The authors are grateful to Suzanne Danley (West Virginia University, USA) for reviewing and editing the manuscript. This work was supported by the National Natural Science Foundation of China [31570978, 31771063, 81702146, 81320108018, 31570943]; National Institutes of Health (NIH) [AR067747–01A1] and an Established Investigator Grant from Musculoskeletal Transplant Foundation (MTF) to Ming Pei; and Priority Academic Program Development of Jiangsu Higher Education Institutions (PAPD).

Abbreviations

ALP	Alkaline phosphatase
AMPK	AMP-activated protein kinase
ARE	antioxidant response element
BGLAP	bone gamma carboxyglutamate protein
BM-MSCs	bone marrow-derived mesenchymal stem cells
CAT	catalase
CC	Compound C
CCK-8	cell counting kit-8
CTRL	control

DCFH-DA	2',7' dichlorofluorescein diacetate
ECM	extracellular matrix
ERK1/2	extracellular-regulated kinase 1/2
FoxO3a	Forkhead box type O transcription factor 3a
GAPDH	glyceraldehyde-3-phosphate dehydrogenase
GPx1	glutathione peroxidase 1
H₂O₂	hydrogen peroxide
MSCs	mesenchymal stem cells
NAC	N-acetyl cysteine
Nrf2	nuclear factor-E2 related factor 2
PBS	phosphate buffered saline
ROS	reactive oxygen species
RUNX2	runt-related transcription factor 2
SIRT1	silent information regulator type 1
SOD	superoxide dismutase
TLR	Toll-like receptor
TNFα	tumor necrosis factor α

References

1. Ozcivici E, Luu YK, Adler B, et al. Mechanical signals as anabolic agents in bone. *Nat Rev Rheumatol* 2010; 6: 50–9. [PubMed: 20046206]
2. Suva LJ, Gaddy D, Perrien DS, et al. Regulation of bone mass by mechanical loading: microarchitecture and genetics. *Curr Osteoporos Rep* 2005; 3: 46–51. [PubMed: 16036101]
3. Smith SM, Zwart SR, Block G, et al. The nutritional status of astronauts is altered after long-term space flight aboard the International Space Station. *J Nutr* 2005; 135: 437–43. [PubMed: 15735075]
4. Ward CW, Prosser BL, Lederer WJ. Mechanical stretch-induced activation of ROS/RNS signaling in striated muscle. *Antioxid Redox Signal* 2014; 20: 929–36. [PubMed: 23971496]
5. Brandes RP, Kreuzer J. Vascular NADPH oxidases: molecular mechanisms of activation. *Cardiovasc Res* 2005; 65: 16–27. [PubMed: 15621030]
6. Ali MH, Pearlstein DP, Mathieu CE, et al. Mitochondrial requirement for endothelial responses to cyclic strain: implications for mechanotransduction. *Am J Physiol Lung Cell Mol Physiol* 2004; 287: L486–96. [PubMed: 15090367]
7. Sart S, Song L, Li Y. Controlling Redox Status for Stem Cell Survival, Expansion, and Differentiation. *Oxid Med Cell Longev* 2015; 2015: 105135. [PubMed: 26273419]
8. Schmelter M, Ateghang B, Helmig S, et al. Embryonic stem cells utilize reactive oxygen species as transducers of mechanical strain-induced cardiovascular differentiation. *FASEB J* 2006; 20: 1182–4. [PubMed: 16636108]

9. Wang K, Zhang T, Dong Q, et al. Redox homeostasis: the linchpin in stem cell self-renewal and differentiation. *Cell Death Dis* 2013; 4: e537. [PubMed: 23492768]
10. Gawlak G, Son S, Tian Y, et al. Chronic high-magnitude cyclic stretch stimulates EC inflammatory response via VEGF receptor 2-dependent mechanism. *Am J Physiol Lung Cell Mol Physiol* 2016; 310: L1062–70. [PubMed: 26993523]
11. Sarsour EH, Kalen AL, Goswami PC. Manganese superoxide dismutase regulates a redox cycle within the cell cycle. *Antioxid Redox Signal* 2014; 20: 1618–27. [PubMed: 23590434]
12. Ji LL. Modulation of skeletal muscle antioxidant defense by exercise: Role of redox signaling. *Free Radic Biol Med* 2008; 44: 142–52. [PubMed: 18191750]
13. Morikawa D, Nojiri H, Saita Y, et al. Cytoplasmic reactive oxygen species and SOD1 regulate bone mass during mechanical unloading. *J Bone Miner Res* 2013; 28: 2368–80. [PubMed: 23674366]
14. Kitada M, Kume S, Imaizumi N, et al. Resveratrol improves oxidative stress and protects against diabetic nephropathy through normalization of Mn-SOD dysfunction in AMPK/SIRT1-independent pathway. *Diabetes* 2011; 60: 634–43. [PubMed: 21270273]
15. Yuan HF, Zhai C, Yan XL, et al. SIRT1 is required for long-term growth of human mesenchymal stem cells. *J Mol Med* 2012; 90: 389–400. [PubMed: 22038097]
16. Yoon DS, Choi Y, Jang Y, et al. SIRT1 directly regulates SOX2 to maintain self-renewal and multipotency in bone marrow-derived mesenchymal stem cells. *Stem Cells* 2014; 32: 3219–31. [PubMed: 25132403]
17. Zhou L, Chen X, Liu T, et al. Melatonin reverses H₂O₂-induced premature senescence in mesenchymal stem cells via the SIRT1-dependent pathway. *J Pineal Res* 2015; 59: 190–205. [PubMed: 25975679]
18. Chen X, Li M, Yan J, et al. Alcohol Induces Cellular Senescence and Impairs Osteogenic Potential in Bone Marrow-Derived Mesenchymal Stem Cells. *Alcohol Alcohol* 2017; 52: 289–97 [PubMed: 28339869]
19. Pardo PS, Mohamed JS, Lopez MA, et al. Induction of Sirt1 by mechanical stretch of skeletal muscle through the early response factor EGR1 triggers an antioxidative response. *J Biol Chem* 2011; 286: 2559–66. [PubMed: 20971845]
20. Liu X, Zhou L, Chen X, et al. Culturing on decellularized extracellular matrix enhances antioxidant properties of human umbilical cord-derived mesenchymal stem cells. *Mater Sci Eng C Mater Biol Appl* 2016; 61: 437–48. [PubMed: 26838870]
21. Zhou L, Chen X, Liu T, et al. SIRT1-dependent anti-senescence effects of cell-deposited matrix on human umbilical cord mesenchymal stem cells. *J Tissue Eng Regen Med* 2018; 12: e1008–e21. [PubMed: 28107614]
22. Song F, Jiang D, Wang T, et al. Mechanical Loading Improves Tendon-Bone Healing in a Rabbit Anterior Cruciate Ligament Reconstruction Model by Promoting Proliferation and Matrix Formation of Mesenchymal Stem Cells and Tendon Cells. *Cell Physiol Biochem* 2017; 41: 875–89. [PubMed: 28214894]
23. Cheng J, Du J. Mechanical stretch simulates proliferation of venous smooth muscle cells through activation of the insulin-like growth factor-1 receptor. *Arterioscler Thromb Vasc Biol* 2007; 27: 1744–51. [PubMed: 17541019]
24. Gao J, Huang T, Zhou LJ, et al. Preconditioning effects of physiological cyclic stretch on pathologically mechanical stretch-induced alveolar epithelial cell apoptosis and barrier dysfunction. *Biochem Biophys Res Commun* 2014; 448: 342–8. [PubMed: 24699412]
25. Tan J, Kuang W, Jin Z, et al. Inhibition of NFκB by activated c-Jun NH2 terminal kinase 1 acts as a switch for C2C12 cell death under excessive stretch. *Apoptosis* 2009; 14: 764–70. [PubMed: 19430970]
26. Gawri R, Rosenzweig DH, Krock E, et al. High mechanical strain of primary intervertebral disc cells promotes secretion of inflammatory factors associated with disc degeneration and pain. *Arthritis Res Ther* 2014; 16: R21. [PubMed: 24457003]
27. Jia LX, Zhang WM, Zhang HJ, et al. Mechanical stretch-induced endoplasmic reticulum stress, apoptosis and inflammation contribute to thoracic aortic aneurysm and dissection. *J Pathol* 2015; 236 373–83. [PubMed: 25788370]

28. Pimentel DR, Amin JK, Xiao L, et al. Reactive oxygen species mediate amplitude-dependent hypertrophic and apoptotic responses to mechanical stretch in cardiac myocytes. *Circ Res* 2001; 453–60.
29. Dick AS, Ivanovska J, Kantores C, et al. Cyclic stretch stimulates nitric oxide synthase-1-dependent peroxynitrite formation by neonatal rat pulmonary artery smooth muscle. *Free Radic Biol Med* 2013; 61: 310–9. [PubMed: 23619128]
30. Lee SK, Min KS, Kim Y, et al. Mechanical stress activates proinflammatory cytokines and antioxidant defense enzymes in human dental pulp cells. *J Endod* 2008; 34: 1364–9. [PubMed: 18928848]
31. Pate KM, Sherk VD, Carpenter RD, et al. The beneficial effects of exercise on cartilage are lost in mice with reduced levels of ECSOD in tissues. *J Appl Physiol* 2015; 118: 760–7. [PubMed: 25593283]
32. Li R, Chen B, Wang G, et al. Effects of mechanical strain on oxygen free radical system in bone marrow mesenchymal stem cells from children. *Injury* 2011; 42: 753–7. [PubMed: 21145545]
33. Hollander J, Fiebig R, Gore M, et al. Superoxide dismutase gene expression is activated by a single bout of exercise in rat skeletal muscle. *Pflugers Arch* 2001; 442: 426–34. [PubMed: 11484775]
34. Koike M, Nojiri H, Ozawa Y, et al. Mechanical overloading causes mitochondrial superoxide and SOD2 imbalance in chondrocytes resulting in cartilage degeneration. *Sci Rep* 2015; 5: 11722. [PubMed: 26108578]
35. Li M, Yan J, Chen X, et al. Spontaneous up-regulation of SIRT1 during osteogenesis contributes to stem cells' resistance to oxidative stress. *J Cell Biochem* 2018. doi: 10.1002/jcb.26730
36. Lee SI, Park KH, Kim SJ, et al. Mechanical stress-activated immune response genes via Sirtuin 1 expression in human periodontal ligament cells. *Clin Exp Immunol* 2012; 168: 113–24. [PubMed: 22385246]
37. Kim MY, Lim JH, Youn HH, et al. Resveratrol prevents renal lipotoxicity and inhibits mesangial cell glucotoxicity in a manner dependent on the AMPK-SIRT1-PGC1alpha axis in db/db mice. *Diabetologia* 2013; 56: 204–17. [PubMed: 23090186]
38. Olmos Y, Sanchez-Gomez FJ, Wild B, et al. SirT1 regulation of antioxidant genes is dependent on the formation of a FoxO3a/PGC-1alpha complex. *Antioxid Redox Signal* 2013; 19: 1507–21. [PubMed: 23461683]
39. Guan XH, Liu XH, Hong X, et al. CD38 Deficiency Protects the Heart from Ischemia/Reperfusion Injury through Activating SIRT1/FOXOs-Mediated Antioxidative Stress Pathway. *Oxid Med Cell Longev* 2016; 2016: 7410257. [PubMed: 27547294]
40. Huang K, Huang J, Xie X, et al. Sirt1 resists advanced glycation end products-induced expressions of fibronectin and TGF-beta1 by activating the Nrf2/ARE pathway in glomerular mesangial cells. *Free Radic Biol Med* 2013; 65: 528–40. [PubMed: 23891678]
41. Tseng PC, Hou SM, Chen RJ, et al. Resveratrol promotes osteogenesis of human mesenchymal stem cells by upregulating RUNX2 gene expression via the SIRT1/FOXO3A axis. *J Bone Miner Res* 2011; 26: 2552–63. [PubMed: 21713995]
42. Lee YM, Shin SI, Shin KS, et al. The role of sirtuin 1 in osteoblastic differentiation in human periodontal ligament cells. *J Periodontol Res* 2011; 46: 712–21. [PubMed: 21745208]
43. Li M, Yan J, Chen X, et al. Spontaneous up-regulation of SIRT1 during osteogenesis contributes to stem cells' resistance to oxidative stress. *J Cell Biochem* 2018; 119: 4928–44. [PubMed: 29380418]
44. Ho PJ, Yen ML, Tang BC, et al. H2O2 accumulation mediates differentiation capacity alteration, but not proliferative decline, in senescent human fetal mesenchymal stem cells. *Antioxid Redox Signal* 2013; 18: 1895–905. [PubMed: 23088254]
45. Choi YJ, Lee JY, Chung CP, et al. Cell-penetrating superoxide dismutase attenuates oxidative stress-induced senescence by regulating the p53-p21(Cip1) pathway and restores osteoblastic differentiation in human dental pulp stem cells. *Int J Nanomedicine* 2012; 7: 5091–106. [PubMed: 23049256]
46. Shi Y, Li H, Zhang X, et al. Continuous cyclic mechanical tension inhibited Runx2 expression in mesenchymal stem cells through RhoA-ERK1/2 pathway. *J Cell Physiol* 2011; 226: 2159–69. [PubMed: 21520068]

47. Tan J, Xu X, Tong Z, et al. Decreased osteogenesis of adult mesenchymal stem cells by reactive oxygen species under cyclic stretch: a possible mechanism of age related osteoporosis. *Bone Res* 2015; 3: 15003. [PubMed: 26273536] .

Author Manuscript

Author Manuscript

Author Manuscript

Author Manuscript

Highlights

- Mechanical stretch induces antioxidant responses in BM-MSCs.
- Intracellular ROS formation is attenuated by cyclic stretch.
- Stretch-mediated antioxidant effect is via activation of AMPK and SIRT1.
- Appropriate stretch promotes osteogenic differentiation of BM-MSCs.
- Excessive stretch has an adverse effect on cellular antioxidant system.

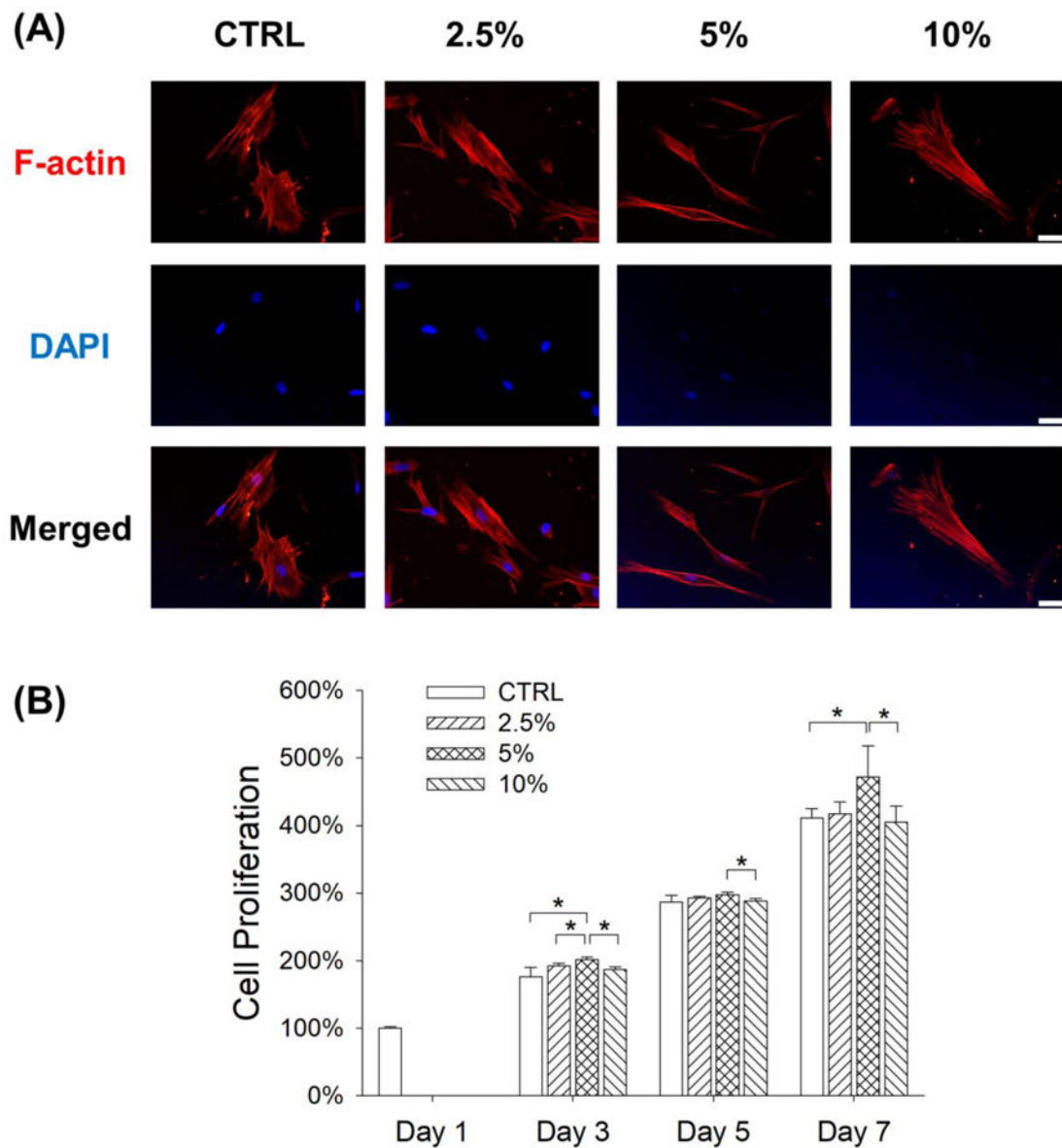


Figure 1.

Effects of mechanical stretch on cell morphology and proliferation of BM-MSCs. Cells were subjected to cyclic stretch for 3 days (2 h per day) at the magnitudes of 2.5%, 5%, and 10%. Cells cultured under static conditions served as the control (CTRL). (A) Cell cytoskeleton F-actin was labeled by rhodamine phalloidin. Longitudinal stretch induced BM-MSCs toward a slender and spindle-like cell shape. Scale bar = 100 μ m. (B) Cell proliferation was quantified at days 1, 3, 5, 7. Data are presented as the mean \pm S.E.M. of four independent experiments ($n = 4$). Statistically significant differences are indicated by * $p < 0.05$ between the indicated groups.

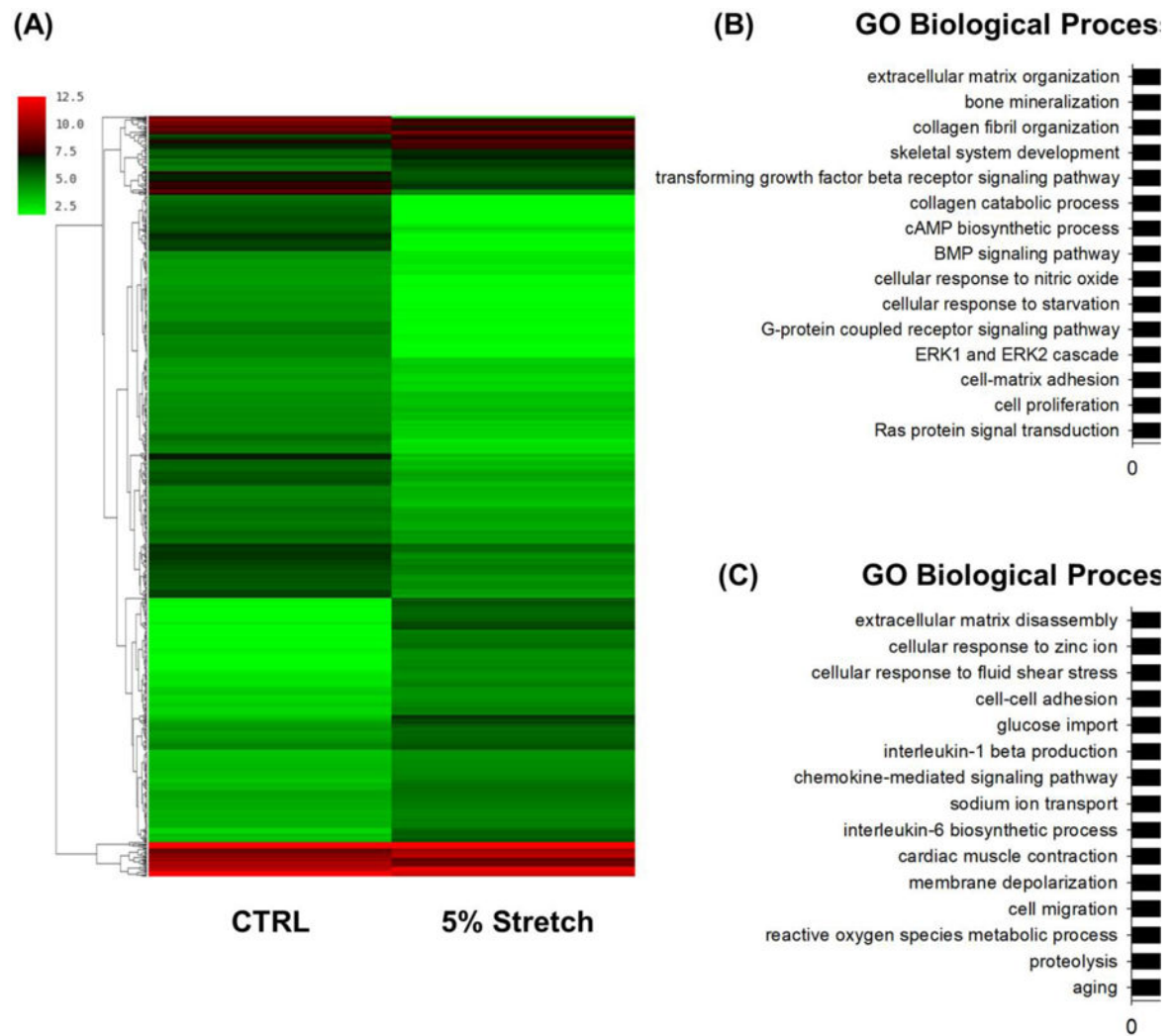


Figure 2.

Global gene expression profile of stretch-treated and static BM-MSCs. Cells were exposed to cyclic stretch of 5% for 3 days and gene expression was analyzed by cDNA microarray. Cells cultured under static conditions served as the control (CTRL). (A) The differently expressed genes in BM-MSCs in response to mechanical stretch are illustrated as a heat map. The color bars on the left of the heat map indicate gene expression level, with redder being higher and greener being lower. (B) GO analysis of the up-regulated gene clusters in stretch-treated BM-MSCs compared with static cells. (C) GO analysis of the down-regulated gene clusters in stretch-treated BM-MSCs compared with static cells.

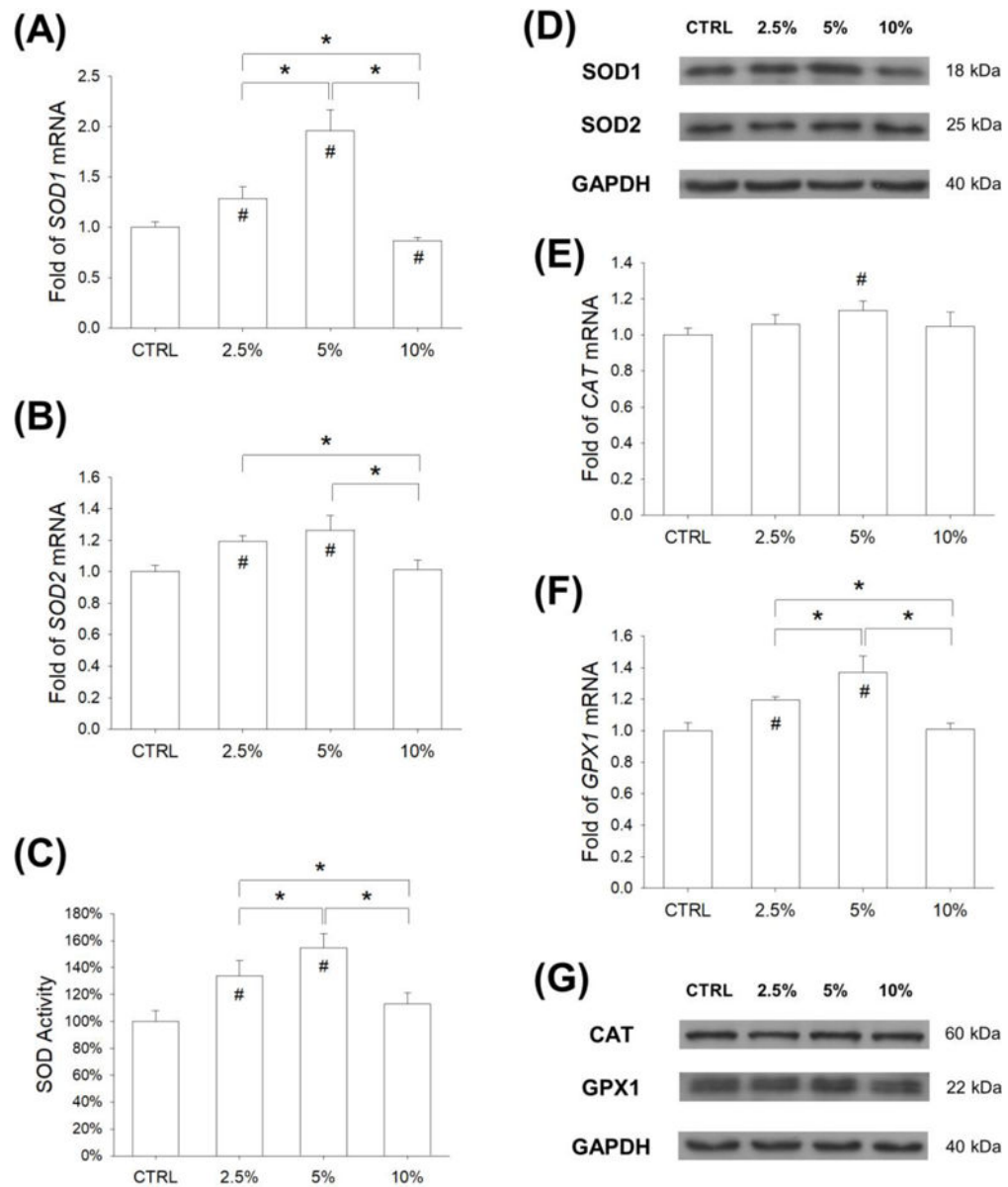


Figure 3.

Effects of mechanical stretch on the levels of intracellular antioxidant enzymes in BM-MSCs. Cells were subjected to cyclic stretch for 2 h per day at the magnitudes of 2.5%, 5%, and 10%. Cells cultured under static conditions served as the control (CTRL). (A-B) After 3 days of stretch, the mRNA levels of *SOD1* (A) and *SOD2* (B) in BM-MSCs were quantified using RT-qPCR. (C) Effects of cyclic stretch on the activity of SOD in BM-MSCs. (D) The protein levels of SOD1 and SOD2 in stretch-treated BM-MSCs were determined by western blot. (E-F) The mRNA levels of *CAT* and *GPX1* (F) in BM-MSCs were quantified using RT-qPCR. (G) The protein levels of CAT and GPx1 in stretch-treated BM-MSCs were determined by western blot. Data are presented as the mean \pm S.E.M. of four independent experiments ($n = 4$) in RT-qPCR and SOD activity experiments. Statistically significant

differences are indicated by * where $p < 0.05$ between the indicated groups and # where $p < 0.05$ vs. the CTRL group.

Author Manuscript

Author Manuscript

Author Manuscript

Author Manuscript

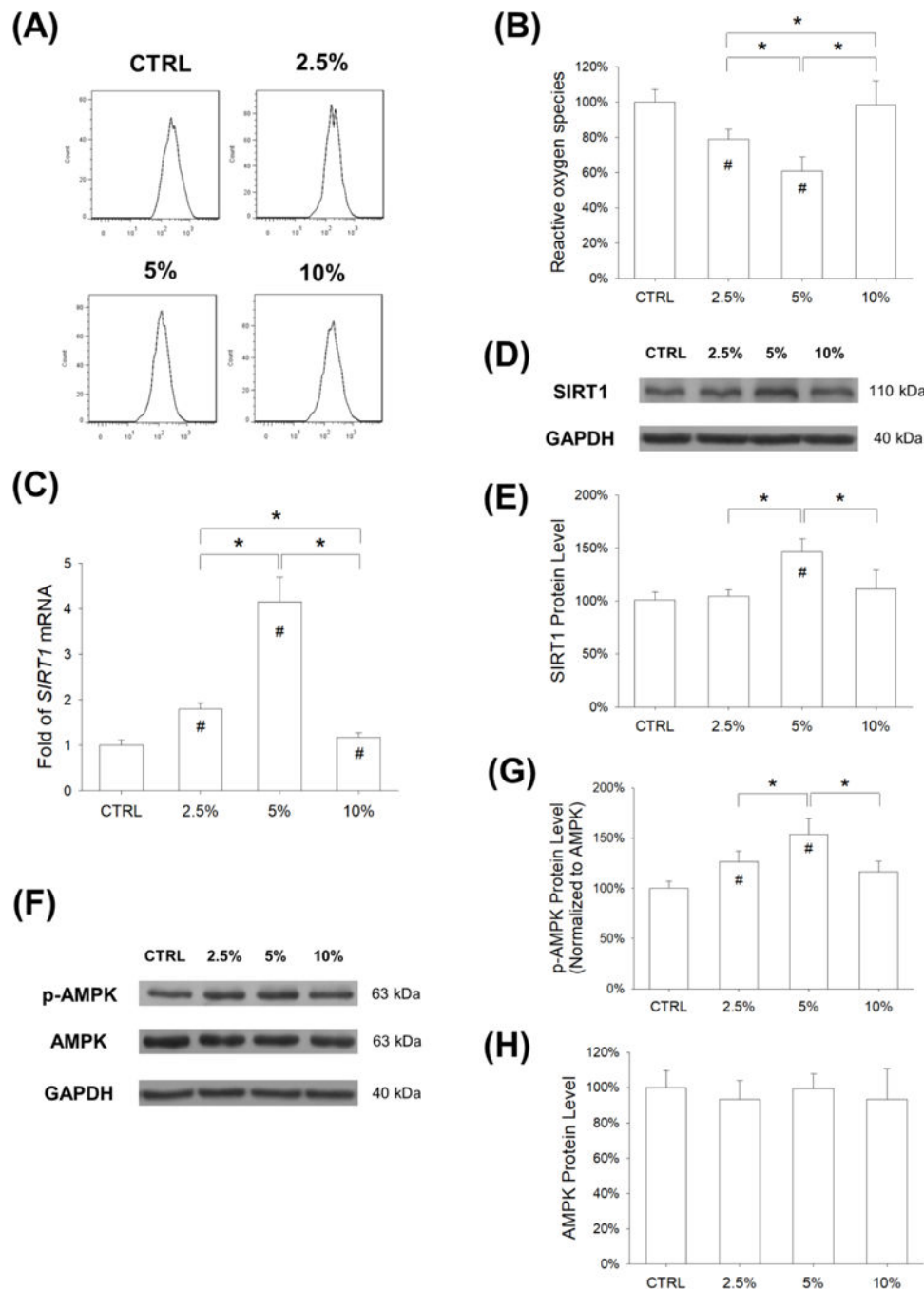


Figure 4. Stretch-induced antioxidant effect on BM-MSCs was through activation of the AMPK-SIRT1 signaling pathway. Cells were exposed to cyclic stretch for 3 days (2 h per day) at the magnitudes of 2.5%, 5%, and 10%. Cells cultured under static conditions served as the control (CTRL). (A) Intracellular ROS of stretch-treated BM-MSCs were determined by flow cytometry. (B) Quantification data showed that cyclic stretch of 2.5% and 5% attenuated the levels of intracellular ROS in BM-MSCs. Data are presented as the mean \pm S.E.M. of four independent experiments ($n = 4$) in ROS assays. (C) The mRNA levels of

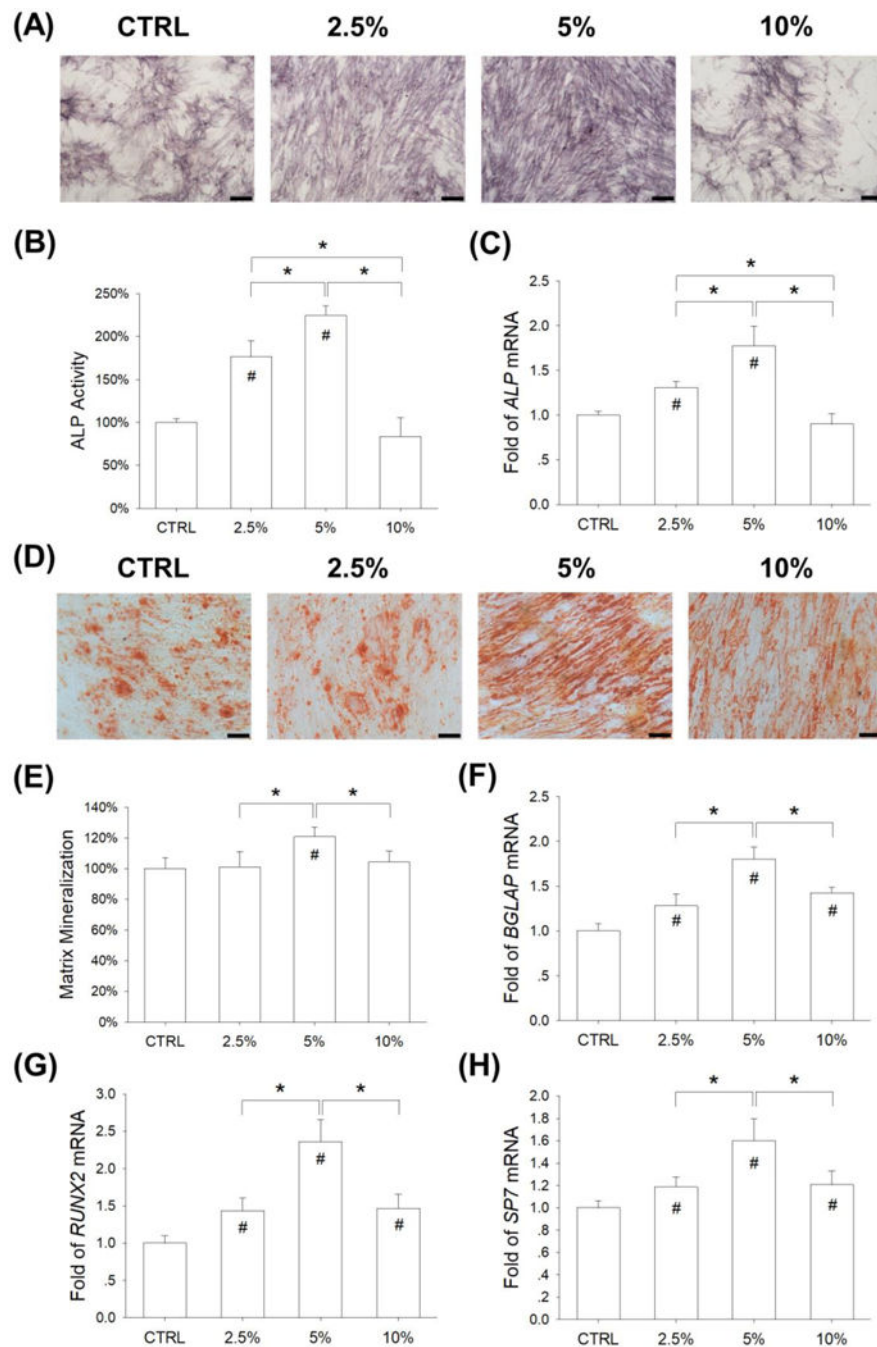
SIRT1 in BM-MSCs were quantified using RT-qPCR. Data are presented as the mean \pm S.E.M. of four independent experiments ($n = 4$) in RT-qPCR experiments. (D-E) The protein levels of SIRT1 in BM-MSCs were determined using western blot assays. (F-G) The phosphorylation levels of AMPK in BM-MSCs were determined using western blot assays. Data are presented as the mean \pm S.E.M. of three independent experiments ($n = 3$) in western blot assays. Statistically significant differences are indicated by * where $p < 0.05$ between the indicated groups and # where $p < 0.05$ vs. the CTRL group.

Author Manuscript

Author Manuscript

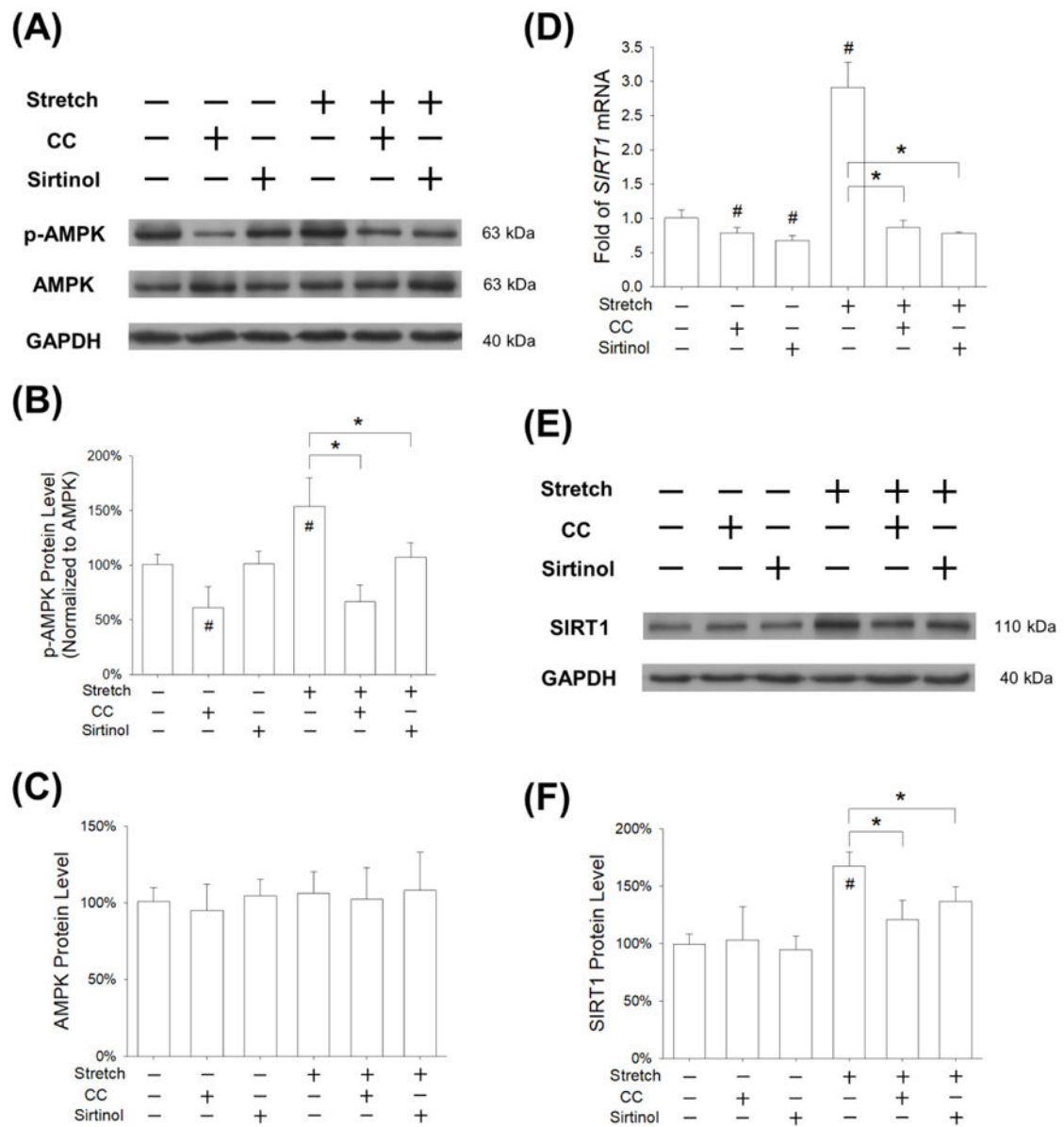
Author Manuscript

Author Manuscript

**Figure 5.**

Effects of mechanical stretch on the osteogenic differentiation of BM-MSCs. Cells were exposed to cyclic stretch for 2 h per day at the magnitudes of 2.5%, 5%, and 10%. Cells cultured under static conditions served as the control (CTRL). (A) After a 7-day induction, intracellular alkaline phosphatase (ALP) stain was used as a marker of the early stage of osteogenesis. Scale bar = 200 μ m. (B) Quantification of ALP activity in stretch-treated BM-MSCs. (C) The mRNA levels of ALP in stretch-treated BM-MSCs were quantified using RT-qPCR. (D) After 14 days of osteogenic differentiation, matrix mineralization was stained

using Alizarin Red S. Scale bar = 200 μm . (E) Quantification of the stained mineral layers in stretch-treated BM-MSCs. (F-H) The mRNA levels of late-differentiated osteoblast marker genes, including *BGLAP* (F), *RUNX2* (G), and *SP7* (H) were quantified using RT-qPCR. Data are presented as the mean \pm S.E.M. of four independent experiments ($n = 4$) in ALP activity, Alizarin Red S staining, and RT-qPCR experiments. Statistically significant differences are indicated by * where $p < 0.05$ between the indicated groups and # where $p < 0.05$ vs. the untreated cells.

**Figure 6.**

Effects of pre-treatment with Compound C (CC) or Sirtinol on stretch-activated AMPK-SIRT1 signaling pathway. BM-MSCs were pre-treated with 10 μ M CC (an AMPK inhibitor) or 40 μ M Sirtinol (a SIRT1 inhibitor) for 2 h, and then subjected to cyclic stretch of 5% for 3 days (2 h per day). (A) The phosphorylation levels of AMPK were measured by western blot assays. (B-C) Quantification of phosphorylation levels and total expression of AMPK in BM-MSCs. (D) The mRNA levels of *SIRT1* were quantified using RT-qPCR. Data are presented as the mean \pm S.E.M. of four independent experiments ($n = 4$) in RT-qPCR experiments. (E-F) The protein levels of SIRT1 were quantified by western blot assays. Data are presented as the mean \pm S.E.M. of three independent experiments ($n = 3$) in western blot assays. Statistically significant differences are indicated by * where $p < 0.05$ between the indicated groups and # where $p < 0.05$ vs. the untreated cells.

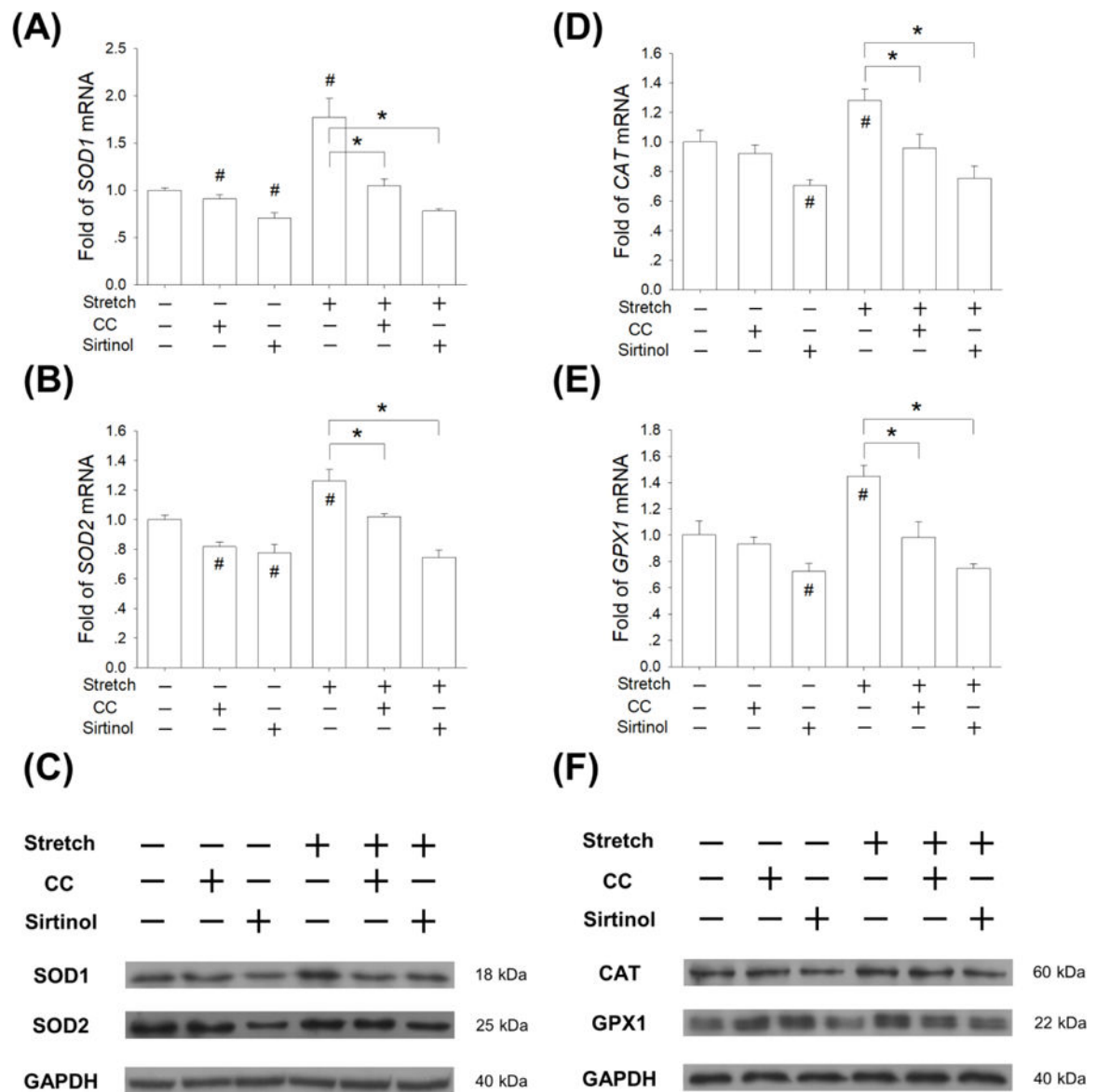
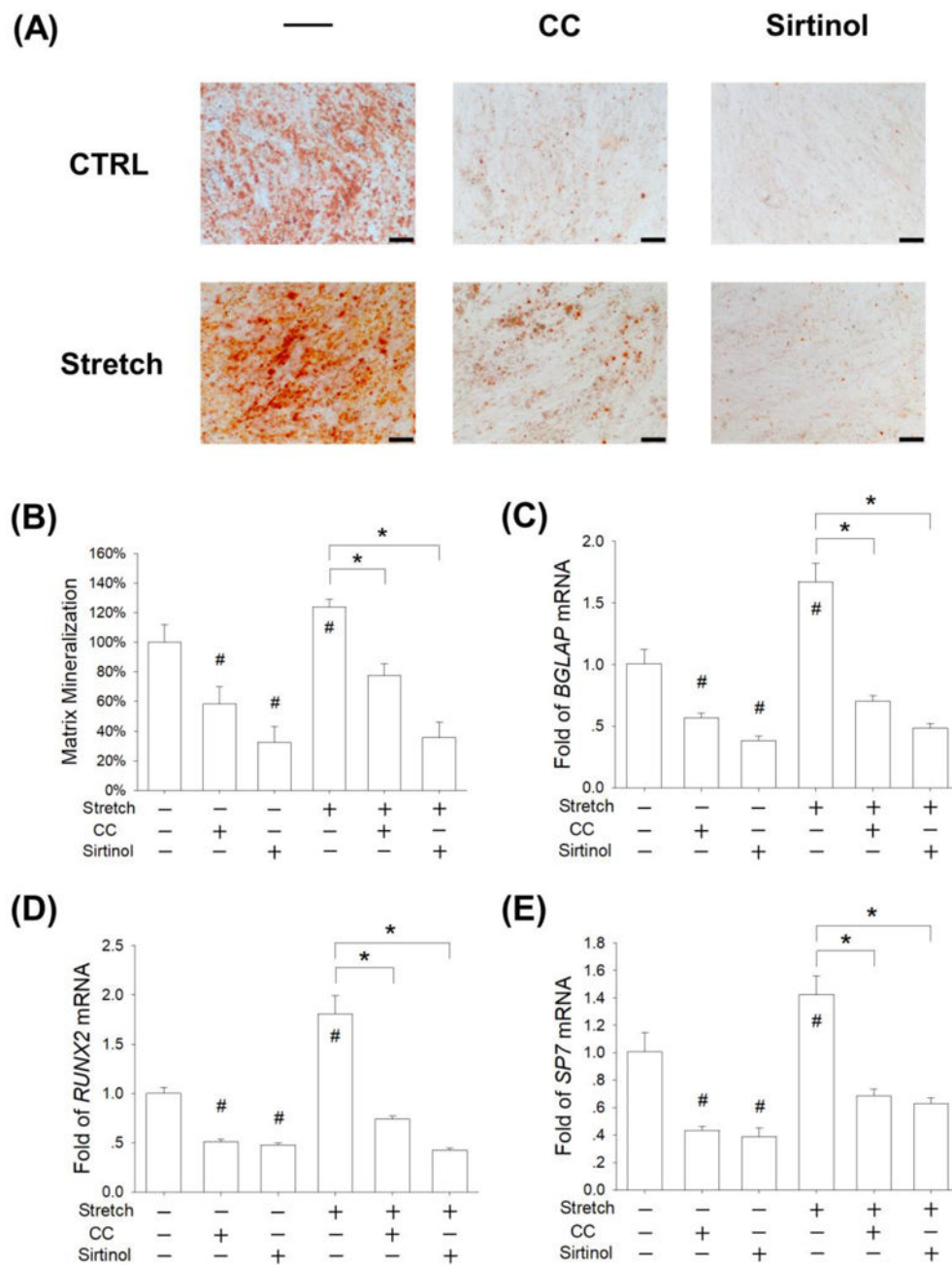


Figure 7. Inhibition of AMPK or SIRT1 abrogated stretch-induced antioxidant responses in BM-MSCs. Cells were pre-treated with CC or Sirtinol for 2 h, and then subjected to cyclic stretch of 5% for 3 days (2 h per day). (A-D) The mRNA levels of *SOD1* (A), *SOD2* (B), *CAT* (C), and *GPX1* (D) in BM-MSCs were quantified using RT-qPCR. Data are presented as the mean \pm S.E.M. of four independent experiments ($n = 4$) in RT-qPCR experiments. (E-F) The protein levels of SOD1, SOD2, CAT, and GPx1 in BM-MSCs were determined using western blot assays. Statistically significant differences are indicated by * where $p < 0.05$ between the indicated groups and # where $p < 0.05$ vs. the untreated cells. Data are presented as the mean \pm S.E.M. of three independent experiments ($n = 3$) in western blot assays. Statistically significant differences are indicated by * where $p < 0.05$ between the indicated groups and # where $p < 0.05$ vs. the untreated cells.

**Figure 8.**

Inhibition of AMPK or SIRT1 suppressed the osteogenic differentiation of stretch-treated BM-MSCs. Cells were incubated in osteogenic differentiation medium supplemented with 10 μ M CC (an AMPK inhibitor) or 40 μ M Sirtinol (a SIRT1 inhibitor) and were exposed to cyclic stretch for 2 h per day at the magnitude of 5%. Cells cultured under static conditions served as the control (CTRL). (A) After 14 days of osteogenic differentiation, matrix mineralization was stained using Alizarin Red S. Scale bar = 200 μ m. (B) Quantification of the stained mineral layers in differentiated BM-MSCs. (C-E) The mRNA levels of late-differentiated osteoblast marker genes, including *BGLAP* (C), *RUNX2* (D), and *SP7* (E)

were quantified using RT-qPCR. Data are presented as the mean \pm S.E.M. of four independent experiments ($n = 4$) in Alizarin Red S staining and RT-qPCR experiments. Statistically significant differences are indicated by * where $p < 0.05$ between the indicated groups and # where $p < 0.05$ vs. the untreated cells.

Table 1.

Primers used for RT-qPCR

Gene	Forward Primer sequence(5'–3')	Reverse Primer sequence(5'–3')
<i>GAPDH</i>	AGAAAAACCTGCCAAATATGATGAC	TGGGTGTCGCTGTTGAAGTC
<i>SOD1</i>	GGTGGGCCAAAGGATGAAGAG	CCACAAGCCAAACGACTTCC
<i>SOD2</i>	GGGGATTGATGTGTGGGAGCACG	AGACAGGACGTTATCTTGTCTGGGA
<i>CAT</i>	TGGGATCTCGTTGAAATAACAC	TCAGGACGTAGGCTCCAGAAG
<i>GPX1</i>	TATCGAGAATGTGGCGTCCC	TCTTGGCGTTCTCTGATGC
<i>SIRT1</i>	GCGGGAATCCAAAGGATAAT	CTGTTGCAAAGGAACCATGA
<i>ALP</i>	AGCACTCCCCTTCATCTGGAA	GAGACCCAATAGGTAGTCCACATTG
<i>BGLAP</i>	GAGCCCCAGTCCCCTACC	GACACCCTAGACCGGGCCGT
<i>RUNX2</i>	AGAAGGCACAGACAGAAGCTTGA	AGGAATGCGCCCTAAATCACT
<i>SP7</i>	CCTCTGCGGGACTCAACAAC	AGCCATTAGTGCTTGTAAGG

Author Manuscript

Author Manuscript

Author Manuscript

Author Manuscript